J. Geomag. Geoelectr., **35**, 473–490, 1983

A Passive Natural-Source Twin-Purpose Borehole Technique: Vertical Gradient Magnetometry (VGM)

Alan G. JONES*

Geophysics Laboratory, Physics Department,
University of Toronto,
Toronto, Ontario, Canada

(Received August 15, 1983)

Two major factors hinder mineral exploration at this present time: (1) a conventional resistivity borehole log is often more indicative of the resistivity of the pore-filled fractured rock in the close locale (< 1 m) of the borehole than the actual resistivity of the layer in which the probe is located; and (2) ground-based em techniques, both natural and controlled source, are often unable to locate a mineralized zone beneath another mineralized zone.

In this paper, the theory is presented for the basis of a conceptually new type of borehole technique based on the ratio of the measurement of the natural horizontal magnetic field variation to its gradient with depth, down the hole, viz. $V_{x,d}(\omega) = H_{x,d}(\omega)/(\partial H_{x,d}(\omega)/\partial z)$. Defining the "downhole apparent resistivity", $\rho_a(\omega,d)$ by

$$\rho_a(\omega, d) = \omega\mu_0|V_{x,d}(\omega)|^2$$

it is shown that, for a 1*D* earth structure, as ω tends to infinity, then $\rho_a(\omega,d)$ tends to the actual resistivity of the layer in which the probe is located. Also, $\rho_a(\omega,d)$ is *independent,* in the 1*D* case, of any structure above it, and weakly dependent in the 2*D* case. The technique has the benefit of most borehole methods of being far superior at resolving structure at depth below it, e.g., a second good-conducting zone, than equivalent ground-based methods (e.g., MT and /or GDS).

Application of the technique to some theoretical 1*D* and 2*D* structures is presented, as well as a discussion of the feasibility of constructing the necessary sensor for the proposed technique.

1. Introduction

Natural electromagnetic prospecting induction methods have one major advantage over controlled source em techniques; namely that they do not require an em source but rely totally on the time variations of the geomagnetic field due to thunderstorm activity—in the 10–10^4 Hz range of frequencies—and

*Present address; Earth Physics Branch, Energy Mines and Resources, Ottawa, Canada, K1A OY3.

ionospheric current variations—in the 10^{-1}–10^{3} s range of periods. Hence, far less equipment is required in the field and problems with cable breaks and transmitter malfunctions are totally avoided. However, to date only surface methods have utilized this superiority—most notably the magnetotelluric (*MT*) technique. Natural source methods have yet to find appeal in airborne or borehole studies.

The *MT* method is well-known to be problematic in regions where the surface rocks have a very high electrical resistivity, for example in Precambrian shield regions. This is due, in the main, to very severe local distortion of the telluric field yielding virtually impossible the task of interpreting the data in terms of reasonable geoelectric models. Also, electrical disturbances propagate over very large horizontal distances due to lack of attenuation in the surface layers and hence there is a high noise content in the data.

In borehole resistivity logging, many problems are encountered with the active probe devices currently in use. Also, these devices are only capable of describing the electrical resistivity in the close vicinity of the borehole—which may be highly atypical of the true "regional" electrical resistivity due to either rock fracture, or pore water movement, caused by the drilling procedure itself.

Another commonly encountered problem in geophysical prospecting is the situation in which one ore body lies beneath another. For example, in such a stratigraphic trap as an anticline. Surface surveys may be insensitive to the presence of the lower conducting zone due to a shielding effect caused by the higher zone.

In this paper, a conceptually new type of borehole geophysical technique is described which both employs the advantages of using natural em variations as its source, and which attempts to address the three problems listed above. The technique, named "*Vertical Gradient Magnetometry" (VGM)*, relies on the attenuation of the natural horizontal magnetic field as it diffuses downward through the earth. The ratio of this attenuation to its gradient with depth is shown herein to be analagous to the *MT* impedance, and accordingly a *downhole VGM apparent resistivity* is defined.

The *VGM* apparent resistivity, $\rho_a(\omega,d)$, is a function of both frequency and depth, hence for any borehole there are many data sets possible to constrain the inversion used to obtain the compatible geoelectric structure. Thus *VGM* is superior to *MT*. Also, *VGM* does not require measurement of the telluric field, hence avoiding all problems associated with this observation.

The *VGM* apparent resistivity has a high frequency asymptote which gives the true electrical resistivity of the layer in which the probe is located. However, the electrical resistivity will be indicative of a "large" horizontal distance around the probe—where "large" here means of the order of a skin depth, δ, given by $\delta = \sqrt{2\rho/\omega\mu}$, in the medium of resistivity ρ. Hence, the *VGM* technique can detail the "regional" value of electrical resistivity.

Also, it will be shown that the *VGM* method is, in a 1*D* earth, insensitive to conductivity structure above it. In 2*D* and 3*D* this is not true, but 2*D* numerical modelling indicates that the probe is more sensitive to structure below it than to structure above it.

Consideration is also given to the feasibility of constructing the necessary sensor, as are solutions to some potential practical difficulties that would arise in its operation.

2. Theory

In the following section, the theory applicable to a layered earth, in which the electrical conductivity is a function of depth alone, i.e., $\sigma(z)$, for the attenuation of the horizontal magnetic field, and its gradient with depth, will be developed. The electric field in layer j is characterized by

$$E_{x_j}(\omega) = A_j \exp(i\omega t - \gamma_j z) + B_j \exp(i\omega t + \gamma_j z) \tag{1}$$

where A_j and B_j are the layer constants pertaining to the downward and upward travelling waves respectively, and γ_j is the layer wave propagation constant given by $\gamma_j^2 = i\omega\mu\sigma_j$ (here it is assumed that the source is uniform, that the magnetic permeability of the medium is that of free space, i.e., $\mu = \mu_0 = 4\pi 10^{-7}\ \mathrm{TmA}^{-1}$, and that displacement currents may be neglected). A third layer constant, C_j, will be of use, defined by

$$C_j = \coth^{-1}\left(\frac{\gamma_j}{\gamma_{j+1}} \coth(C_{j+1})\right) + \gamma_j h_j \tag{2}$$

where h_j is the thickness of the j 'th layer, with $C_n = \infty$, where n is the number of layers. The magnetic field in the layer is derived from curl $E = -i\omega\mu H_y$ hence

$$H_{y_j}(\omega) = \frac{\gamma_j}{i\omega\mu}[A_j \exp(i\omega t - \gamma_j z) - B_j \exp(i\omega t + \gamma_j z)] \tag{3}$$

(a) Uniform half-space. In a half-space of uniform conductivity σ, the horizontal magnetic field $H_y(\omega)$ attenuates with depth in the well-known exponential manner, so that the ratio of the field observed at depth d, $H_{y,d}(\omega)$, to the field at the surface, $H_{y,0}(\omega)$, is given by

$$\frac{H_{y,d}(\omega)}{H_{y,0}(\omega)} = \exp(-\gamma d) \tag{4}$$

This is because $B_n = 0$, i.e., there is not an upward travelling wave from a half space. Taking the gradient of this attenuation with depth z gives

$$\frac{\partial}{\partial z}\left(\frac{H_{y,d}(\omega)}{H_{y,0}(\omega)}\right) = -\gamma \exp(-\gamma d) \tag{5}$$

Obviously, the ratio of the field at depth d to its gradient at that same depth, defined as the Vertical Gradient Magnetometry response function $V_{y,d}(\omega)$, is given by

$$V_{y,d}(\omega) = \frac{H_{y,d}(\omega)}{\partial H_{y,d}(\omega)/\partial z} = -\frac{1}{\gamma} \tag{6}$$

Defining the depth and frequency dependent *VGM apparent resistivity* and *phase* functions by

$$\rho_a(\omega, d) = \omega\mu_0 |V_{y,d}(\omega)|^2 \tag{7}$$

and

$$\phi(\omega, d) = \tan^{-1}\left(\frac{\mathrm{Im}(V_{y,d}(\omega))}{\mathrm{Re}(V_{y,d}(\omega))}\right) \tag{8}$$

it is obvious that in the half space the *VGM apparent resistivity* $\rho_a(\omega,d)$ gives the true electrical resistivity $\rho = 1/\sigma$ at all depths d and all frequencies ω. The phase function $\varphi(\omega, d)$ is, for all depths and frequencies, constant and equal to $\tan^{-1}(1/-1) = 3\pi/4$.

(b) Two-layered earth. Consider the earth consisting of a layer of conductivity σ_1, with its associated wave propagation constant γ_1 and layer constants A_1, B_1 and C_1, and thickness h_1, overlying a uniform half-space of conductivity σ_2, propagation constant γ_2 and layer constants A_2 and $C_2(=\infty)$ (note $B_2 = 0$). Obviously, from Eq. (2), C_1 is given by

$$C_1 = \coth^{-1}\left(\frac{\gamma_1}{\gamma_2}\right) + \gamma_1 h_1 \tag{9}$$

There are two possible layers in which to measure $V_{y,d}$, i.e., $d < h_1$ and $d > h_1$. For $d < h_1$, then the measuring point is within the top layer and the attenuation of the horizontal magnetic field is given by

$$\left(\frac{H_{y,d}}{H_{y,0}}\right)_{d<h_1} = \frac{A_1 \exp(-\gamma_1 d) - B_1 \exp(+\gamma_1 d)}{A_1 - B_1} \tag{10a}$$

$$= \frac{\sinh(C_1 - \gamma_1 d)}{\sinh(C_1)} \tag{10b}$$

The gradient with depth of this attenuation is given by

$$\left(\frac{\partial}{\partial z}\left(\frac{H_{y,d}}{H_{y,0}}\right)\right)_{d<h_1} = \frac{-\gamma_1 \cosh(C_1 - \gamma_1 d)}{\sinh(C_1)} \tag{11}$$

and hence $(V_{y,d})_{d<h1}$ is given by

$$(V_{y,d})_{d<h_1} = \frac{-1}{\gamma_1 \coth(C_1 - \gamma_1 d)} \tag{12a}$$

$$= \frac{-\left(\frac{\gamma_1}{\gamma_2} + \coth(\gamma_1(h_1 - d))\right)}{\gamma_1\left(\frac{\gamma_1}{\gamma_2}\coth(\gamma_1(h_1 - d)) + 1\right)} \tag{12b}$$

For ω large and $(h_1 - d)$ not small, then $\coth(\gamma_1(h_1 - d)) \to 1$ and hence

$$(V_{y,d})_{\substack{d<h_1 \\ \omega \text{ large}}} \to -\frac{1}{\gamma_1} \tag{13}$$

$$(\rho_a(\omega, d))_{\substack{d<h_1 \\ \omega \text{ large}}} \to \rho_1 \tag{14}$$

$$(\phi(\omega, d))_{\substack{d<h_1 \\ \omega \text{ large}}} \to \frac{3\pi}{4} \tag{15}$$

For ω small, and/or $(h_1 - d)$ small, then $\coth(\gamma_1(h_1 - d)) \to \infty$ and

$$(V_{y,d})_{\substack{d<h_1 \\ \omega \text{ small} \\ h_1 - d \text{ small}}} \to -\frac{\gamma_2}{\gamma_1^2} \tag{16}$$

$$(\rho_a(\omega, d))_{\substack{d<h_1 \\ \omega \text{ small} \\ h_1 - d \text{ small}}} \to \frac{\rho_1^2}{\rho_2} \tag{17}$$

$$(\phi(\omega, d))_{\substack{d<h_1 \\ \omega \text{ small} \\ h_1 - d \text{ small}}} \to \frac{3\pi}{4} \tag{18}$$

For $d > h_1$ then the attenuation in the lower half-space is given by

$$\left(\frac{H_{y,d}}{H_{y,0}}\right)_{d>h_1} = \left(\frac{H_{y,d}}{H_{y,h_1}}\right)_{d>h_1}\left(\frac{H_{y,h_1}}{H_{y,0}}\right) \tag{19a}$$

$$= \exp(-\gamma_2(d - h_1))\frac{\sinh(C_1 - \gamma_1 h_1)}{\sinh(C_1)} \tag{19b}$$

and its gradient is given by

$$\left(\frac{\partial}{\partial z}\left(\frac{H_{y,d}}{H_{y,0}}\right)\right)_{d>h_1} = \exp(-\gamma_2(d - h_1))\frac{-\gamma_2 \sinh(C_1 - \gamma_1 h_1)}{\sinh(C_1)} \tag{20}$$

Hence

$$(V_y(\omega, d))_{d>h_1} = -\frac{1}{\gamma_2} \tag{21}$$

and therefore the *VGM* response function in the lower half space acts as if there does not exist an upper layer.

(c) *N*-layered Earth. The above expressions for $V_y(\omega, d)$ can be generalized for an *n*-layered earth. For measurements of a horizontal component of the magnetic field, and its gradient, in the *j*'th layer then the attenuation of the magnetic field compared to its surface value is given by

$$\left(\frac{H_{y,d}}{H_{y,0}}\right)_{d_{j-1}<d<d_j} = \frac{\sinh(C_j - \gamma_j d')}{\sinh(C_j)} \prod_{k=1}^{j-1} \frac{\sinh(C_k - \gamma_k h_k)}{\sinh(C_k)} \tag{22}$$

where d_j is the depth to the *j*'th interface, i.e., $d_j = \Sigma_k{}^j{}_{=1} h_k$ and d' is the height of the measurement above the *j*'th interface, i.e., $d' = d_j - d$. Obviously,

$$\left(\frac{\partial}{\partial z}\left(\frac{H_{y,d}}{H_{y,0}}\right)\right)_{d_{j-1}<d<d_j} = \frac{-\gamma_j \cosh(C_j - \gamma_j d')}{\sinh(C_j)} \prod_{k=1}^{j-1} \frac{\sinh(C_k - \gamma_k h_k)}{\sinh(C_k)} \tag{23}$$

and the *VGM* response function is given by

$$(V_y(\omega, d))_{d_{j-1}<d<d_j} = \frac{-1}{\gamma_j \coth(C_j - \gamma_j d')} \tag{24}$$

The following points about the *VGM* response function for a 1*D* earth are worthy of note:

(i) the response function $(V_y(\omega, d))_{d_{j-1}<d<d_j}$ is only dependent on the parameters of the layer in which the measurement is being made and those below it — it is independent of the parameters of any of the layers above it.

(ii) for $d = 0$, i.e., for measurements made at the surface of the earth, then

$$V_y(\omega, 0) = \frac{-1}{\gamma_1 \coth(C_1)} \tag{25a}$$

$$= \frac{1}{\sigma_1 Z_{xy}(\omega)} \tag{25b}$$

$$= \frac{1}{i\omega\mu\sigma_1 C(\omega)} \tag{25c}$$

where $Z_{xy}(\omega)$ and $C(\omega)$ are the MT impedance and Schmucker's inductive response functions respectively.

(iii) The *VGM* apparent resistivity, as given by Eq. (7), in the j'th layer has the following asymptotes at high and low frequencies

$$\lim_{\omega \to \infty} (\rho_a(\omega, d)) = \rho_j \tag{26a}$$

$$\lim_{\omega \to 0} (\rho_a(\omega, d)) = \frac{\rho_j^2}{\rho_n} \tag{26b}$$

(assuming $d \neq d_j$, i.e., $d' \neq 0$). Asymptote (26b) is also reached as $d \to d_j$, i.e., $d' \to 0$.

3. Examples

In this section, two models will be studied which illustrate the potential uses of the proposed *VGM* borehole technique. The first example is a 1*D* model—the response functions are derived analytically from standard *MT* theory and the theory presented in the previous section. The second example is more geophysically meaningful in as much as it considers a 2*D* model—the *VGM* and surface *MT* responses are derived numerically. For both models considered, the significant parameters are determined by application of a *Singular Value Decomposition (SVD)* of the Jacobian matrix relating infinitesimally small variations in the model parameters to the changes introduced on the calculated response functions (see, for example, EDWARDS *et al.*; 1981, JONES, 1982). Also, the model parameter inter-correlations are derived by the techniques described in INMAN (1975). The models will be studied in the framework of *MT* geophysical surveys, of increasing complexity, being undertaken over them. The surveys will be: (1) a single station *scalar MT*, i.e., 1 station estimating apparent resistivities only, with a standard deviation of 25%, in the frequency range $10 - 10^3$ Hz; followed by (2) a 5 station tensor *MT* survey, of standard deviations of 10% in apparent resistivity and 3^0 in phase, in the frequency range $10 - 10^4$ Hz; (3) a re-interpretation of the tensor *MT* data with known *a priori* information, obtained from a 50 m deep borehole, included; finally (4) a *VGM* probe lowered through the borehole and measurements made of the *VGM* apparent resistivity and phase in the frequency range $10 - 10^4$ Hz, with associated standard deviations of 10% and 3^0 respectively.

(a) 1*D* model. Consider the 5-layer 1*D* model illustrated in Fig. 1a of two highly conducting zones, 16 m thick of layer electrical resistivity $\rho = 10$ Ωm and at depths of 24 m and 100 m, in an otherwise uniform half space, of known host resistivity $\rho = 10^3$ Ωm. As shown in Fig. 1b, the theoretical *MT* apparent resistivity and phase responses for this model are discernably different from those that would be observed if the lower conducting layer did not exist.

An *SVD* analysis of the Jacobian matrix for this particular model, with

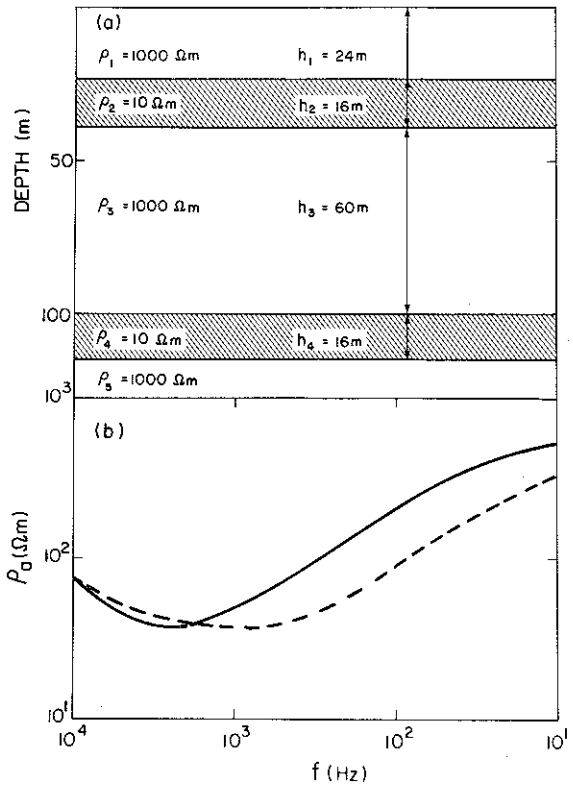

Fig. 1. (a) the 1*D* geoelectric model considered in this study; (b) the surface *MT* apparent resistivity response for the model illustrated in (a) *(dashed line)*, and for the model without the lower conducting layer *(full line)*.

an assumed standard deviation in apparent resistivity of 25%, yields the information given in Table 1. (As mentioned above, the resistivity of the host is assumed to be known, hence ρ_1, ρ_3, and ρ_5 are problem constants and not problem variables.) It can be seen in Table 1 that of the six problem variables, i.e., the four thicknesses h_1, h_2, h_3, and h_4, and the resistivities of the two conducting zones, i.e., ρ_2 and ρ_4, only two eigenparameters — or "mixed" model parameters — can be estimated from the data set. The most sensitive parameter of the problem is a mixed parameter which represents the depth-integrated conductivity of the upper conducting layer, $h_2\sigma_2$(conductivity-thickness product). This eigenparameter has an associated singular value of 15, which implies that it can be well estimated from the data. The only other eigenparameter that can be estimated from the *AMT* information is a mixture of most of the model parameters, i.e., $h_1h_3h_3\sigma_4/\sigma_2$, and has an associated singular value of 4.6, hence is barely resolveable. Also, the model parameter h_2 highly correlates (0.96) with the parameter h_4. In conclusion therefore, although the scalar *AMT* survey would

Table 1. SVD analyses of the 1*D* model and significant model parameter inter-correlations.

Survey	Singular values greater than unity	Associated parameter eigenvectors						Physical interpretation	Significant model parameter inter-correlations
		log (ρ_2)	log (ρ_4)	log (h_1)	log (h_2)	log (h_3)	log (h_4)		
Scalar *AMT*	15	− 60	− 41	− 10	55	− 10	39	Conductivity-thickness of UCL	h_2 & h_4 (0.96)
	4.6	38	− 49	45	− 18	34	52	?	h_3 & h_4 (−.82) h_3 & h_4 (0.82)
Tensor *AMT*	41	− 65	− 33	− 24	55	− 10	31	Conductivity-thickness of UCL	
	27	9	− 33	88	11	− 1	32	Thickness of first layer	h_4 & ρ_4 (−.68) h_3 & h_2 (0.61)
	14	− 35	52	38	31	− 28	− 54	Conductivity-thickness of LCL	h_1 & ρ_2 (−.59)
	4.0	16	− 17	− 10	− 16	− 95	6	Thickness of UCL	
Re-interpreted tensor *MT*	16		71			7	− 70	Conductivity-thickness of LCL	none
	2.3		0			− 99	− 10	Thickness of third layer	
VGM	47		− 66			− 45	60	Conductivity-thickness of LCL	none
	35		28			− 89	− 36	thickness of third layer	

UCL = upper conducting layer. LCL = lower conducting layer.

give information which would reveal the existence of the upper conducting layer, the lower one would be missed.

A tensor *MT* survey in the frequency range 10 – 10^4 Hz over the 1*D* model illustrated in Fig. 1a, with associated standard errors of 10% in apparent resistivity and 3^0 in phase, would yield 4 mixed parameters of the model, as listed in Table 1. The most accurately determined parameter would be $h_2\sigma_2$, the conductivity-thickness product of the upper conducting layer, followed by h_1, $h_4\sigma_4$, and, marginally, h_3 (associated singular value of 4.0). Eigenparameter $h_4\sigma_4$, the depth-integrated conductivity of the lower conducting layer, is independent, i.e., does not correlate with any of the other model parameters. Hence, the tensor *MT* data would reveal the presence of the lower conducting zone, but only through its conductivity-thickness product. The depth to the zone would not be determinable however.

After drilling the structure, a re-interpretation of the tensor *MT* data, with the *a priori* knowledge of h_1, h_2, and ρ_2, would yield 2 eigenparameters, namely $h_4\sigma_4$ *and* h_3 (see Table 1). Hence, the depth to the lower conducting zone could now be determined, but again only its conductivity-thickness product.

For the 1*D* model under consideration, the horizontal magnetic field in the frequency range 10 –10^4 Hz attenuates through the layered structure as indicated by Fig. 2a. The *VGM* apparent resistivity response at these two bounding frequencies is illustrated in Fig. 2b — which displays the "logging" capabilities of the technique. If the probe were lowered to a depth of 50 m, i.e., just below

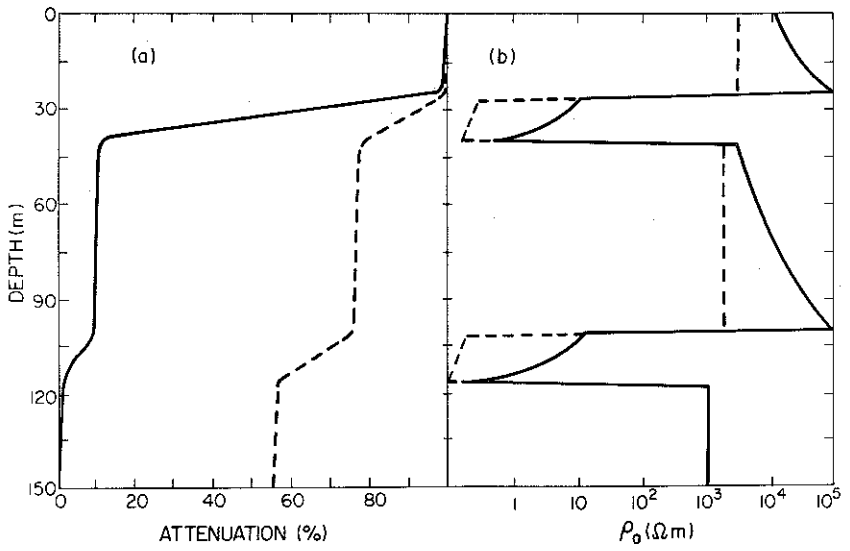

Fig. 2. (a) the attenuation of the horizontal magnetic field, $H_{x,d}(\omega)$, as it diffuses through the model illustrated in Fig. 1a at frequencies of 10^4 Hz *(full line)* and 10 Hz *(dashed line)*; (b) the downhole *VGM* apparent resistivity, $\rho_d(\omega, d)$, for the model illustrated in Fig. 1a at frequencies of 10^4 Hz *(full line)* and 10 Hz *(dashed line)*.

the upper conducting zone, and the response function evaluated, then an interpretation of this response function would yield 2 eigenparameters, as listed in Table 1. These eigenparameters are exactly as for the re-interpretation of the tensor *MT* data, but both are much more accurately resolved (compare the listed singular values in Table 1). The variation of $\rho_a(\omega,d)$ with frequency at a depth of 50 m in the 1*D* model is illustrated in Fig. 4.

(b) 2*D* model. The 2*D* model to be considered is illustrated in Fig. 3a and represents two highly conducting blocks of electrical resistivity $\rho = 10$ Ωm, of dimensions 100 m in width and 16 m thickness, at depths of 24 m and 100 m, in an otherwise uniform half space of host electrical resistivity $\rho = 10^3$ Ωm. Hence, this model is analagous to the 1*D* model with the exception that the zones of increased conductivity are limited in extent in one horizontal dimension.

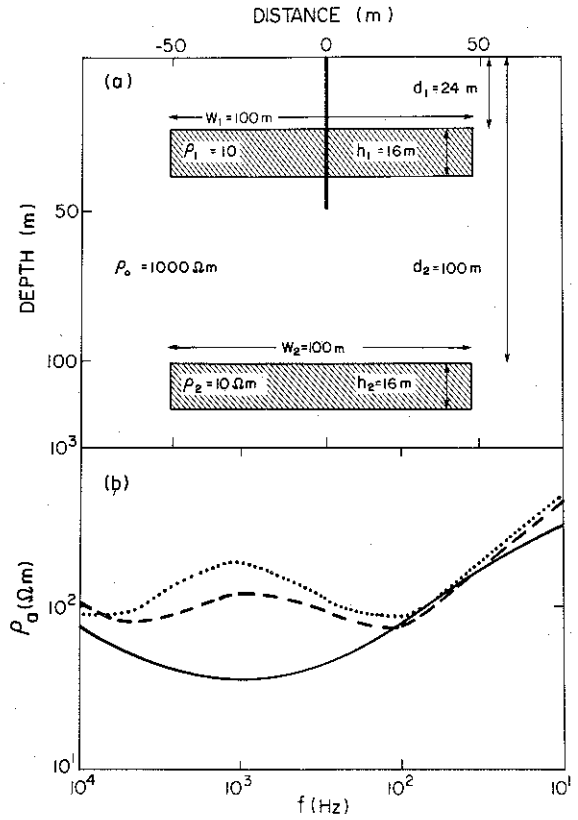

Fig. 3. (a) the 2*D* geoelectric model considered in this study, the solid line at $x = 0$ m to a depth of $z = 50$ m represents the borehole; (b) a comparison of the surface *MT* apparent resistivity responses for the 1*D* model *(full line)* illustrated in Fig. 1a, and the 2*D* model *(dashed line)* illustrated in Fig. 3a. The *dotted line* is the surface *MT* response for the 2*D* model in the absence of the lower conducting zone.

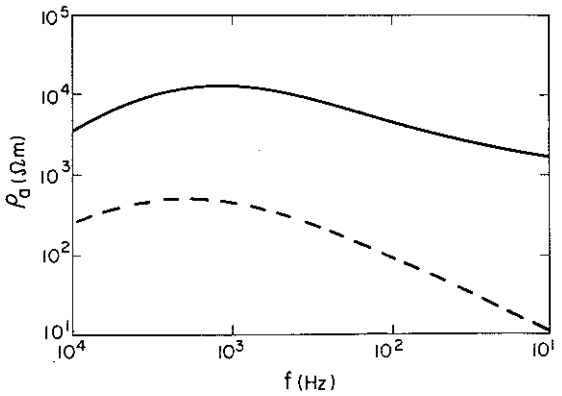

Fig. 4. A comparison of the *VGM* apparent resistivity, $\rho_a(\omega, d)$, observed at the base of the borehole, i.e., at x,z co-ordinates (0,50), for the 1*D* model *(full line)* illustrated in Fig. 1a, and for the 2*D* model *(dashed line)* illustrated in Fig. 3a.

The differences in the surface *MT* responses between this 2*D* model and the 1*D* model are illustrated in Fig. 3b, for both the two-anomaly model and for the upper anomaly existing alone. It is apparent from the figure that for *MT* the discovery of the lower zone demands highly accurate date. As before, it is assumed in the *SVD* analyses that the host resistivity is known and is therefore not a problem variable but a problem constant.

Assuming that, purely fortuitously, the scalar *AMT* survey is conducted above the centre of the anomalies, the eigenparameters, and their associated singular values, of the model that can be derived are listed in Table 2. Also given in Table 2 are the significant model parameter inter-correlations. From the scalar *AMT* data, only two eigenparameters can be deduced, (i) the areal conductivity of the upper body, i.e., width × thickness × conductivity product, $w_1h_1\rho_1$, and (ii) the depth to the lower conducting zone, d_2. It might be considered that from the latter of these two, definitive information was contained in the data to show the existence of the lower body. However, the parameter d_2 correlates with eigenparameter $w_1h_1\sigma_1$, and hence is not independently determinable. Thus, the lower conducting zone would, almost certainly, not be interpreted from the scalar *AMT* data.

However, the survey would show that the upper conducting zone existed, hence a tensor *MT* survery might be undertaken. Tensor *MT* data, with stations located at −230 m, −90 m, 0 m, 90 m and 230 m and with its more accurate apparent resistivity information and phase response, would resolve 5 eigenparameters, as listed in Table 2. The width of the upper conducting zone is best delineated (w_1), followed by d_2, $h_1\sigma_1$ (conductivity-thickness product of the upper zone), d_1, and , marginally, $w_2h_2\sigma_2$, i.e., the areal conductivity of the lower zone. However, as shown in Table 2, all the parameters of the lower zone inter-correlate with mixed parameters of the upper zone. Hence, the lower zone

Table 2. SVD analyses of the 2*D* model and significant model parameter inter-correlations.

Survey	Singular values greater than unity	Associated parameter eigenvectors								Physical interpretation	Significant model parameter inter-correlations
		log (ρ_1)	log (ρ_2)	log (w_1)	log (w_2)	log (d_1)	log (d_2)	log (h_1)	log (h_2)		
Scalar *AMT*	11	− 43	− 14	61	26	− 8	− 49	31	8	Conductivity-thickness-width product of UCZ	All parameters significantly correlate (> 0.75)
	2.4	23	− 3	− 33	3	12	− 84	− 32	− 12	Depth to LCZ	
Tensor *MT*	75	34	6	− 83	− 15	18	30	− 23	− 2	Width of UCZ	ρ_1 & w_1 (−.88)
	33	− 4	− 13	− 30	22	32	− 86	− 4	0	Depth to LCZ	ρ_1 & w_2 (−.81)
	15	55	14	29	− 22	− 25	− 27	− 60	− 21	Conductivity-thickness of UCZ	ρ_1 & h_1 (−.97)
											ρ_2 & w_2 (0.94)
	12	− 33	4	− 37	− 18	− 81	− 22	6	− 8	Depth to UCZ	ρ_2 & d_2 (0.81)
	5	21	− 49	− 3	57	− 32	11	− 22	47	Conductivity-thickness-width of LCZ	w_1 & d_1 (−.71)
											w_1 & h_1 (0.84)
											w_2 & d_2 (−.83)
											w_2 & h_1 (0.76)
Re-interpreted tensor *MT*	67		6	− 92	− 17		35		− 2	Width of UCZ	
	31		− 13	− 39	21		− 89		− 1	Depth to LCZ	
	8.3		43	7	− 69		− 25		− 52	Conductivity-thickness-width of LCZ	ρ_2 & w_2 (−.94) ρ_2 & d_2 (0.81) w_2 & d_2 (−.83) w_1 & w_2 (0.70)
	1.3		− 62	4	− 66		− 8		41	Resistivity-width of LCZ	
VGM	180		− 4	4	12		− 99		4	Depth to LCZ	All parameters significantly correlate (> 0.65)
	72		54	40	− 53		− 9		− 50	Conductivity-thickness-width of LCZ	
	53		− 10	88	44		10		9	Width of UCZ	
	2.1		78	− 21	58		31		4	Resistivity-width of LCZ	
	1.2		− 29	− 14	40		1		− 85	Thickness of LCZ	

UCZ = upper conducting zone. LCZ = lower conducting zone.

would, in all probability, not be interpreted from the tensor *MT* information. The upper zone would be fairly well defined (w_1, $h_1\sigma_1$ and d_1), and thus would be drilled.

A re-interpretation of the tensor *MT* data, with the *a priori* information that $d_1 = 24$ m, $h_1 = 10$ m, and $\rho_1 = 10\Omega$m provided by a borehole log, would be able to delineate eigenparameters w_1, d_2, $w_2h_2\sigma_2$ and, very marginally (singular value of 1.3) $w_2\rho_2$ (the resistivity-width product of the lower conducting zone) respectively. However, w_1 is intercorrelated with $w_2h_2\sigma_2/\ d_2$, and it is possible that the upper body would be interpreted as having an erroneous width, and that the lower body would be missed from the interpretation.

Placing a *VGM* downhole probe at the base of the drilled hole would yield response functions which would be most sensitive to the eigenparameters listed in Table 2. The best determined parameter is the depth to the lower conducting zone, d_2, then $w_2h_2\sigma_2$, w_1, $w_2\rho_2$ and (very marginally) h_2 respectively. The depth to the lower conducting zone is determinable to better than 1%. Note that the *VGM* response for this model displays the characteristic of 1*D* models that it is more sensitive to structure beneath the probe than to structure above it. The *VGM* apparent resistivities, $\rho_a(\omega, d)$, that would be observed at the base of the drill hole for both the 1*D* and the 2*D* models are illustrated in Fig. 4.

4. Feasibility of Construction

The downhole probe for the proposed *VGM* technique will, by necessity, have two magnetic field sensors for each horizontal component. The advantages of having both horizontal *VGM* responses, $V_{x,d}(\omega)$ and $V_{y,d}(\omega)$ far outweigh the increased cost involved. For the type of problem discussed in this paper, i.e., conducting bodies embedded in resistive host media (such as shield areas), in both the 1*D* and the 2*D* cases the gradient of the horizontal magnetic field is of the order of 0.1% - 0.3% of the surface value at a frequency of 10 kHz. At 10 Hz, this gradient drops to 0.01% of the surface field value. Hence, as the natural magnetic field spectrum exhibits typically a magnitude of 100 – 1000 mγ at 10 kHz (SERSON 1973, WARD 1983), the resolution of the sensors has to be to better than 10^{-2} mγ, for a 1 meter coil separation, at these frequencies. At 10 Hz however, the natural spectrum exhibits typically an amplitude of only 10 – 100 mγ, and hence a resolution of 10^{-4} mγ is required.

In situations where the host is relatively conducting, e.g., sedimentary basins, a different frequency range is required due to the higher frequency variations being attenuated in the surface layers. For example, in the Rhinegraben (the Rhine valley), there are sediments of resistivity around 10 Ωm to a depth of 2500 m, overlying a highly resistive basement of 5000 Ωm. For such a model, the high frequencies (10 Hz – 10 kHz) are only useful within the top 100m, below which the gradient of the horizontal magnetic field becomes smaller than 10^{-7} of the surface value. At the much lower frequencies, however, of 10^{-1}–10^{-3} Hz (i.e., 10 – 10^3 s period), the gradients are of the order of 0.5% –

2% of the surface field value within the sedimentary layers (they drop to 10^{-4}% within the resistive basement). At these frequencies, the natural spectrum typically exhibits a field of 0.1 γ (at 10^{-1} Hz) – 10 γ (at 10^{-3} Hz), hence requiring a sensor with a noise level appreciable below 1 mγ (at 10^{-1} Hz) to 100 mγ (at 10^{-3} Hz).

Of the downhole coils known to the author, the most sensitive is that of WORTHINGTON *et al.* (1981). Their horizontal component downhole sensor is constructed to fit within a tube of internal diameter 1 1/4 inches, and is approximately 60 cm total length. It has a quoted noise level of 0.01 mγ $Hz^{-1/2}$. At 10 kHz, and for a reasonable bandwidth of 100 Hz, the RMS noise level is 0.1 mγ, which is an order of magnitude too high. At 10 Hz, and 0.1 Hz bandwidth, the RMS noise level is 10^{-4} mγ, which is about the magnitude of the gradient. The recent patent by VOZOFF (1983) suggests using SQUIDs down boreholes. However, the best available SQUIDs (CLARKE *et al.*, 1983) have exactly the same quoted noise level as the above coils. Hence, unless the bandwidth of these devices (coils or SQUIDs) can be dramatically reduced, by more than two orders of magnitude, direct measurement of the gradient at these high frequencies cannot be made with the present day sensors.

At the lower frequencies, i.e., 10^{-1} – 10^{-3} Hz, there are currently available downhole fluxgate magnetometers with quoted noise levels of 10 mγ $Hz^{-1/2}$. At 10^{-1} Hz, and for a bandwidth of 10^{-3} Hz, this suggests an RMS noise level of the same magnitude as the gradient. At the much lower frequency of 10^{-3} Hz, the gradient should be directly measureable due to the much higher natural signal levels.

However, present day sensors could be employed to determine an ensemble estimate of the response function $V_{y,d}$ by "stacking" the cross-spectra between the gradient and the surface field, and those between the downhole field and the surface field. The estimate would then be given by the "remote reference" formula discussed in the following section.

5. Practical Operation

Several practical problems arise with regard to the operation of the proposed *VGM* probe. One of the most severe is knowledge of the orientation of the probe within the hole. Three different methods are suggested here which could be employed to gain orientation information. The most accurate, but technically the most difficult and expensive, would be to mount a recording gyroscope onto the probe itself. This is already used on larger diameter devices employed in the oil exploration industry. The data from the gyroscope could be multiplexed back up to the surface together with the horizontal field measurements. An alternative approach would be to use a line current source on the surface at the top of the hole, and measure the horizontal fields in both directions down the hole, $[H^s_{x,d}, H^s_{y,d}]$, due to the source. The direction in which this field is a maximum could be taken as the direction of the orientation of the line. This ap-

proach suffers from two main problems; (a) a controlled source is required, which negates one of the principal advantages of the *VGM* technique in that it utilizes natural electromagnetic field variations hence alleviating any requirement for a controlled source; and (b) 3*D* conductivity structures may distort the magnetic field to such an extent that the direction of maximum observable magnitude due to the source may not be the same direction as the line orientation. The third method could be to measure simultaneously the surface natural horizontal magnetic field variations, $[H_{x,0}, H_{y,0}]$, and correlate them with the downhole values $[H'_{x,d}, H'_{y,d}]$ to find angle θ such that $H_{x,d}$ and $H_{y,d}$ given by

$$\begin{bmatrix} H_{x,d} \\ H_{y,d} \end{bmatrix} = \begin{bmatrix} \cos\theta & \sin\theta \\ -\sin\theta & \cos\theta \end{bmatrix} \begin{bmatrix} H'_{x,d} \\ H'_{y,d} \end{bmatrix}$$

maximally correlates with $H_{x,0}$ and $H_{y,0}$ respectively. This technique, as did the previous, also assumes that there is insignificant distortion of the magnetic fields due to 3*D* conductivity structure. However, measurement of $[H_{x,0}, H_{y,0}]$ is advised for the reasons detailed below.

The problem of noise free estimation of $V_{x,d}$ and $V_{y,d}$ from knowledge of $(H_{x,d}, \partial H_{x,d}/\partial z)$ and $(H_{y,d}, \partial H_{y,d}/\partial z)$ can be breduced by measuring the horizontal magnetic fields $[H_{x,0}, H_{y,0}]$ and using these as the "instrumental variables" of the problem. For example, the upward and downward noise-biased estimates, where the "noise" terms are assumed to be uncorrelated with each other and with any signals, of $V_{x,d}$ are given by

$$[\hat{V}_{x,d}]_u = \frac{\langle H^*_{x,d} H_{x,d} \rangle}{\langle H^*_{x,d} G_{x,d} \rangle}$$

and

$$[\hat{V}_{x,d}]_d = \frac{\langle G^*_{x,d} H_{x,d} \rangle}{\langle G^*_{x,d} G_{x,d} \rangle}$$

respectively, where $G_{x,d}$ denotes $\partial H_{x,d}/\partial z$, $\langle\ \rangle$ denotes averaging, and * implies complex conjugate. These forms are well known in *MT*. A noise-unbiased estimate of $V_{x,d}$ is given by

$$[\hat{V}_{x,d}] = \frac{\langle H^*_{x,0} H_{x,d} \rangle}{\langle H^*_{x,0} G_{x,d} \rangle}$$

where it can be recognised that $H_{x,0}$ performs the role of a "remote reference" on $[H_{x,d}, G_{x,d}]$, as introduced to *MT* by GAMBLE *et al.* (1978; see also CLARKE *et al.*, 1983). The importance of a remote reference in problems of transfer function estimation in the presence of noise was first recognised by REIERSØL (1950,

see also Akaike 1967), which he termed the "instrumental variable" of the problem.

6. Conclusions

In this paper, a conceptually new type of borehole technique has been described, and the theory applicable to a 1*D* earth detailed. It has been shown that the method possesses several advantages over both surface *MT* and current downhole resistivity logging tools. The technique utilizes the attenuation of the natural horizontal magnetic field, and its gradient, as it diffuses downward through the earth. It has been shown that the downhole apparent resistivity, $\rho_a(\omega,d)$, is closely related to the *MT* apparent resistivity, and hence the method could be employed in lieu of *MT* in areas where there is an unacceptable amount of noise on the natural telluric field. Alternatively, the *VGM* response could be coupled with surface *MT* information to yield greater constraints on the models, as previously suggested for controlled source work by ORISTAGLIO and WORTHINGTON (1980) and WORTHINGTON *et al.* (1981).

The possible application of the *VGM* technique as a resistivity logging tool has also been displayed. This use arises from the high frequency asymptote of the *VGM* apparent resistivity tending towards the electrical resistivity of the layer in which the probe is located.

Finally, the sensitivity of the technique to below probe structure for 1*D* and 2*D* models has been illustrated.

The author has received financial support from grants awarded to Professor G.D. Garland (NSERCC A2115) and to Professors R.N. Edwards and G.F. West (NSERCC G0501), for which he wishes to acknowledge his deep gratitude.

REFERENCES

AKAIKE, H., Some problems in the application of the cross-spectral method, in *Advanced Seminar on Spectral Analysis of Time Series*, edited by B. Harris, pp. 81–107, John Wiley and Sons Ltd., 1967.

CLARKE, J., T. D. GAMBLE, W. M. GOUBAU, R. H. KOCH, and R. F. MIRACKY, Remote reference magnetotellurics: equipment and procedures, *Geophys. Prospect.*, **31**, 149–170, 1983.

EDWARDS, R. N., R. C. BAILEY, and G. D. GARLAND, Conductivity anomalies: lower crust or asthenosphere?, *Phys. Earth Planet. Inter.*, **25**, 263–272, 1981.

GAMBLE, T. D., W. M. GOUBAU, and J. CLARKE, Magnetotellurics with a remote reference, *Geophysics*, **44**, 53–68, 1978.

INMAN, J. R., Resistivity inversion with ridge regression, *Geophysics*, **40**, 798–817, 1975.

JONES, A. G., On the electrical crust-mantle structure in Fennoscandia: No Moho and the asthenosphere revealed? *Geophys. J. R. Astr. Soc.*, **68**, 371–388, 1982.

ORISTAGLIO, M. L. and M. H. WORTHINGTON, Inversion of surface and borehole electromagnetic data for two-dimensional electrical conductivity models, *Geophys. Prospect.*, **28**, 633–657, 1980.

REIERSØL, O., Identifiability of a linear relation between variables which are subject to error, *Econometrica*, **18**, 375–389, 1950.

SERSON, P. H., Instrumentation for induction studies on land, *Phys. Earth Planet. Inter.*, **7**, 313–322, 1973.

VOZOFF, K., Superconducting gradiometer-magnetometer array for magnetotelluric logging (U.S. Patent No. 4,349,781), *Geophysics*, **48**, 252, 1983.

WARD, S., Controlled source em methods: a review, *Geophys. Surv.*, 1983, submitted (presented as a review paper at the 6th Workshop).

WORTHINGTON, M. H., A. KUCKES, and M. ORISTAGLIO, A borehole induction procedure for investigating electrical conductivity structure within the broad vicinity of a hole, *Geophysics*, **46**, 65–67, 1981.